

Real-time mapping of an industrial flare using LIDAR

Renata F. da Costa^a, Juliana Steffens^b, E. Landulfo^a, Roberto Guardani^b, W. M. Nakaema^a,
Paulo F. Moreira Jr.^b, Fabio J. S. Lopes^a and Patrícia Ferrini^a

^aIPEN-CLA, Avenida Prof. Lineu Prestes 2242, São Paulo, Brazil, 05508-00;

^bEscola Politécnica da Universidade de São Paulo, Av. Luciano Gualberto 380 Tr 3, São Paulo, Brazil, 05508-970

ABSTRACT

Characterization of atmospheric emissions from industrial flare stacks represents a challenge in measurement techniques because it is extremely difficult to determine the real-time concentrations of combustion products by in situ sampling, due to stack height, sensor calibration difficulties, and the dynamics of oscillations in the emission patterns. A ground based laser remote sensing (LIDAR) system has been developed for continuous and real-time monitoring of atmospheric emissions from an oil refinery located approximately 400 m from the instrument. The system is able to perform 3D scanning and profiling around the emission point. Tests were carried out using a scanning system pointed to the refinery flare. The mapping was obtained from a sequence of measurements at different zenithal and azimuthal angles resulting in a 3D image of the flare shape plus the flame itself. The measurements can be used to estimate the aerosol size distribution based on the ratios of the backscattering signal at three distinct wavelengths: 1064/532 nm, 1064/355 nm, and 532/355 nm. The method can be used in real time monitoring of industrial aerosol emissions and in the control of industrial processes. Preliminary results indicate a calibration procedure to assess the refining process efficiency based on the particle size distribution within and around the flare.

Keywords: LIDAR, petrochemical flare, mapping, aerosol size distribution

1. INTRODUCTION

A sensor for air pollution monitoring should allow for on site, continuous, and unattended operation over a long period of time, preferably achieved by an instrument with a simple and robust design.¹ In this aspect, optical remote sensing techniques have significant advantages for gas and particle pollutant detection over conventional systems, which are usually based on sampling and measurement by a train of analytical devices. Optical methods show important advantages in this aspect: on-line evaluation of the measurement, no contamination of samples and the possibility of measuring large areas.² Optical remote sensing devices based on LIDAR (light detection and ranging) technique are relatively simpler in construction, and enable real time detection of changes in optical response over large distances, in hostile environments with large fluctuations of temperature and pressure. These features enable the technique to be applied to the monitoring of emissions from industrial processes involving fast change of physical-chemical composition and phase.³

The study presented here was carried out in the industrial area of the city of Cubatão, in the Southeast of Brazil, located at the Atlantic coast, ca. 50 km from São Paulo, and one of the largest industrial sites in the country. In a region with ca. 40 km² there are 23 large industries, including a steel plant, an oil refinery, 7 fertilizer plants, a cement plant, and 11 chemical/petrochemical plants, adding up to 260 pollutant emission sources, besides the urban area, with ca. 130 thousand inhabitants.⁴ The LIDAR system was installed ca. 400 m far from one of the industrial flare stacks, which has a total height of ca. 40 m relative to the ground level. The stack location relative to the LIDAR was about 30° east from the geographical north, which is aligned with the most frequent wind direction, which comes mainly from ca. 200° - 230°, or S/SW, according to local records. An illustrative map of the region is shown in Figure 1.

Further author information: (Send correspondence to Renata F. da Costa)
Renata F. da Costa: E-mail: renata.facundes.costa@usp.br, Telephone: 55 11 3133-9255

The LIDAR system performed systematic scanning measurements around the flare and registered the time evolution of the backscattered light at three wavelengths, namely 1064 nm radiation from a Nd:YAG lasers and its second and third harmonics, 532 and 355 nm, respectively. The preliminary results indicate a strong dependence of the intensity patterns on the wavelength of the incident light, which is apparently can be associated with the emission patterns of aerosol particles and other scattering sources by the combustion process in the flare. In this text the equipment and measuring methods are described, and illustrative results are presented and discussed.



Figure 1. Location of Cubatão, LIDAR System and Flare site.

2. MATERIALS AND METHODS

2.1 LIDAR Set-up

The LIDAR system employed in this study is a three-wavelength backscattering system operating in the biaxial mode. The light source is a commercial Nd:YAG laser (CFR 450, Quantel SA) operating at 355 nm, 532 nm, and 1064 nm with a fixed repetition rate of 20 Hz. The emitted laser pulses have a divergence of less than 0.3 mrad. The receiving module is a 150 mm diameter Dall-Kirkham telescope and focal length of 1000 mm used to collect the backscattered laser light. The LIDAR is currently used with a fixed field of view (FOV) of 1 mrad, which permits a full overlap between the telescope FOV and the laser beam at heights around 90 m away the LIDAR system. This FOV value, in accordance with the detection electronics, enables sampling at distances up to 7 km. A picture of the system is show in Figure 2(a).

The backscattered laser radiation is detected by two photomultiplier tubes (Hamamatsu) and one Si-avalanche photodiode (EG&G) coupled to narrowband interference filters to assure the reduction of the solar background during daytime operation and to improve the signal-to-noise ratio (SNR). The PMT output signal is recorded by a Transient Recorder in both analog and photocounting mode.

The laser plus telescope devices are attached to a scanning base adapted from a 2 AP sun tracker that performs changes in both azimuthal and polar angles with an accuracy of less than 0.02 degrees. This system has two stepper motors controlled by an on-board micro-computer to program a full scanning over a desired angle range. The main features of the system are summarized in table 1.

2.2 Data collection

All data were collected in a period of approximately one hour. A 12 x 12 virtual matrix was created in front of the flare flame and the first cell of that matrix was generated at a zenithal angle equal to 12.30° and an azimuthal

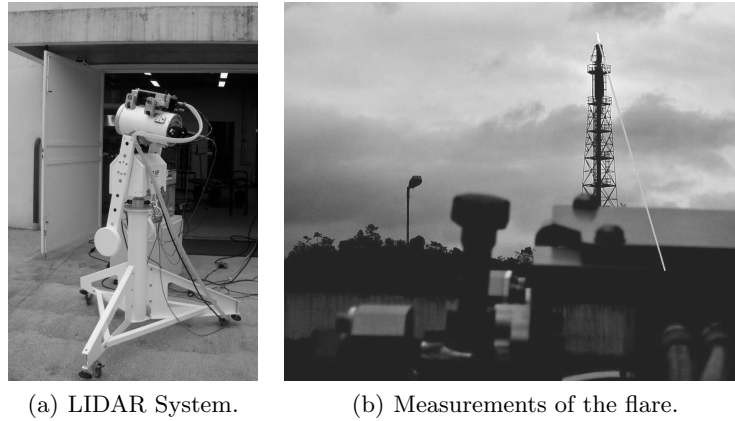


Figure 2. LIDAR System operation during the sampling sequence. The white line has been drawn in order to enhance the laser beam to improve visualization.

Table 1. LIDAR system features.

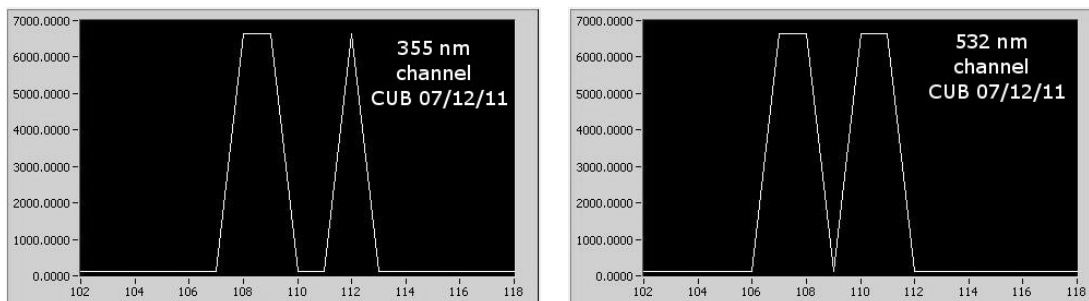
Laser	
Laser type	Nd:YAG Laser (ICE 450/CFR)
Wavelengths	355, 532, 1064 nm
Pulse energy	100 mJ (at 355 nm), 200 mJ (at 532 nm) and 400 mJ (at 1064 nm)
Repetition rate	20 Hz
Pulse duration	(7 ± 2) ns
Receiver	
Optical design	150 mm diameter cassegranian telescope
Focal length	1000 mm
Field of view	≤ 1 mrad
Transient recorder	Licel (TR20-80) 10 - 250 MHz bandwidth

angle equal to 25.88° . The variations of the zenithal and azimuthal angles were made in steps of 0.03 and 0.04 degrees, respectively, until the system reached the end of the scan at the position $\Delta\theta$ of 0.33 and $\Delta\phi$ of 0.48 degrees. According to these values, the flame height was estimated in 1.89 m. During the acquisition for each cell of the matrix, the integration time was fixed in 10 seconds. Only the cells presenting more than 17,000 counts in the 355 nm channel were considered as originated from the flame itself due to the larger molecular scattering in this wavelength. The 1064 nm channel was used as a sensor for aerosol particles generated as a product of the combustion or recombination of other compounds surrounding the flame. The 532 nm channel represents the transition between the two channels since it is associated with both molecular and particulate scattering. The ratio between the wavelength dependent backscattered signals, especially 1064/355, can be used to estimate the size distribution of the aerosol particles.

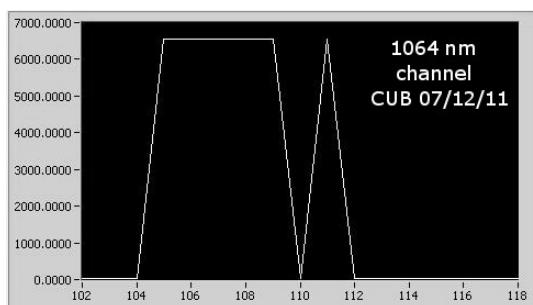
2.3 Data analysis

For each individual cell of the matrix, the intensity provided from the integrated range-corrected backscattering LIDAR signal (equation 1) was used to map and distinguish the flame occurrence from its surroundings. The indexes r_1 and r_2 in the summation represent the limits adopted by considering the sequence of bins which showed highest intensity of the collected signal, i.e., approximately 3.75 m before and after the flame according to the bin width observed. Figure 3 shows the raw photocounting signal between bins 102 and 118. We also can see from the figure the highest intensity signal is around bins 106 and 112.

$$I_{i,j}(\lambda, r) = \sum_{r_1}^{r_2} [P_{i,j}(\lambda, r) r^2] \quad (1)$$



(a) Bin by bin channel 355 obtained by Hamamatsu's PMT. (b) Bin by bin channel 532 obtained by Hamamatsu's PMT.



(c) Bin by bin channel obtained by 1064 EG&G 's APD.

Figure 3. Bin by bin of LIDAR system channels sampling display. Bin 102 represents a distance of 382.5 m from the LIDAR system to the flare. In the same way, 118 represents a distance of 442.5 m. The integration time was fixed in 10 seconds.

The normalized intensity (equation 2) for two wavelengths can indicate the occurrence of specific scattering sources in the flame. For example, the ratio 1064/355 can point out the larger presence of aerosols over the sampled area.

$$RI_{i,j} = \frac{I_{i,j}(\lambda_1, r)}{I_{i,j}(\lambda_2, r)} \quad (2)$$

3. RESULTS

Figures 4, 5 and 6 show the intensity of integrated range-corrected backscattering LIDAR signal around the stack flame at 355 nm, 532 nm and 1064 nm respectively, in arbitrary units. The stack is aligned with the bottom line of each plot. According to the total angular displacement of 0.24 degree and the distance between the flare and the LIDAR system, the base of the flame was estimated as being ca. 1.4 m wide, and its height was estimated as ca. 1.9 m. The figures correspond to a monitoring campaign carried out on June 12 of 2011, under clear sky condition, from 16:40 to 17:36 h, wind from 230° and average velocity of 0.23 m/s. Thus, the flame products were being transported away from the monitoring place. The shape of the flame for the 355 nm and 532 nm channels is relatively well delimited, probably due to the more efficient Rayleigh scattering,⁵ while at 1064 nm the Mie scattering is expected to be more pronounced, leading to a spreading of the intensity distribution that makes it difficult to define the corresponding flame dimension. On the other hand, the response at this last channel (Figure 6) can be used to indicate the spatial distribution of aerosol particles around the flare flame. The plots for the three wavelengths indicate that smaller scattering sources (molecules) concentrate close to the

stack (ca. 408 - 412 m), while high concentration of aerosol particles have been detected at larger distances, as far as 40 m from the flame.

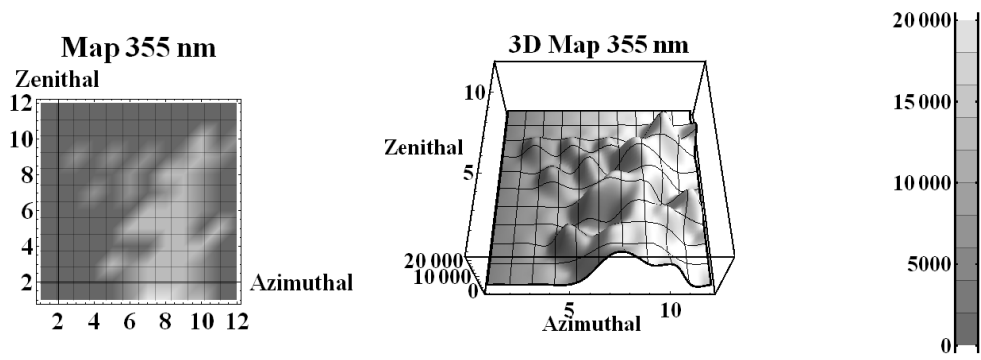


Figure 4. Scattering intensity at 355 nm (arbitrary units). The flare stack is situated at ca. 400 m.

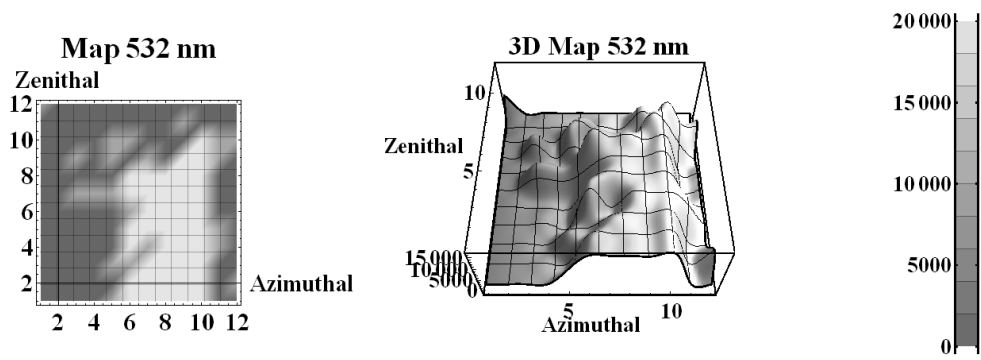


Figure 5. Scattering intensity at 532 nm (arbitrary units). The flare stack is situated at ca. 400 m.

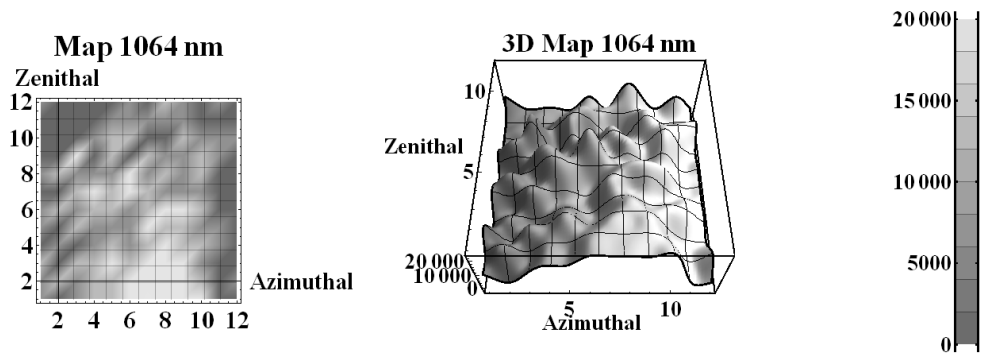


Figure 6. Scattering intensity at 1064 nm (arbitrary units). The flare stack is situated at ca. 400 m.

The spatial distribution of scattering sources of different species is evidenced in Figures 7 and 8, which show the signal ratio corresponding to 1064/355 and 1064/532 respectively, for the plane situated at 412.5 m from the monitoring place, i.e., close to the stack opening. In both plots, the brighter cells, indicating larger values of the ratio, are observed at larger distances from the stack opening. This distribution is in agreement with

the expected behavior in flares, since aerosol particles (e.g., water droplets, soot) buildup at certain distances from the flame, while higher concentration of molecules of the emitted gas normally concentrate near the stack opening, where combustion takes place. The spatial distribution of the ratios is less homogeneous in Figure 7 (1064/355 ratio) than in Figure 8 (1064/532 ratio).

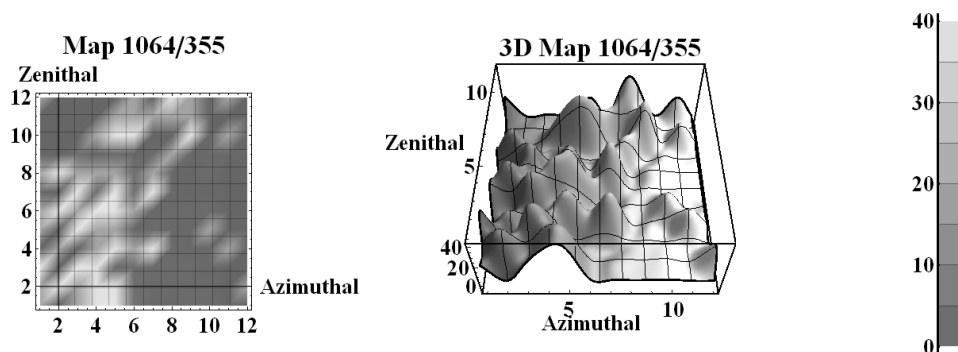


Figure 7. Ratio between 1064/355 channels

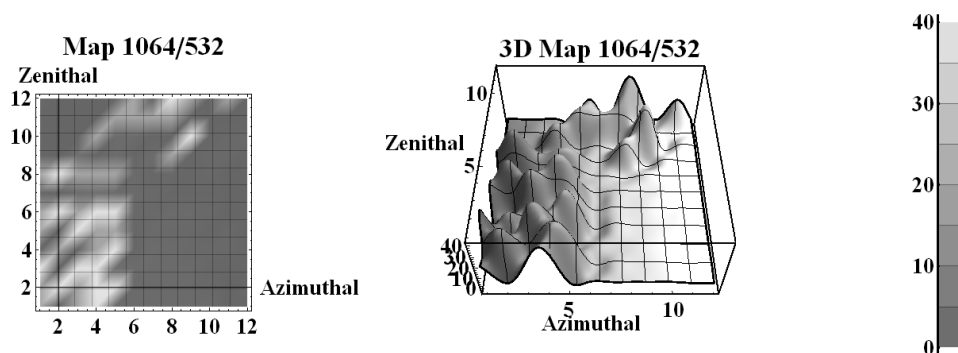


Figure 8. Ratio between 1064/532 channels

4. CONCLUSIONS

The results of the monitoring campaign with the directional LIDAR device indicate that the technique can be used in real time monitoring of the spatial distribution of emitted species from industrial stacks. By processing the scattering signal at different wavelengths or wavelength ratios, additional information can be obtained concerning the spatial distribution and the characteristics of the different scattering sources that may be emitted or formed in flare flames. This information may represent a valuable tool in prediction of dispersion characteristics of industrial atmospheric emissions, and, when coupled with information on the wind field and other meteorological variables, can be used to validate dispersion models.

In order to develop a quantitative monitoring device, further studies shall be carried out focused on the calibration of the system and correlation with operating variables from the industrial process in each case.

ACKNOWLEDGMENTS

The financial support by the agencies FAPESP and CNPq, as well as by CEPEMA (Environmental Research Center of the University of São Paulo), and by Petrobras is kindly acknowledged by the authors.

REFERENCES

- [1] Linnerud, I., Kaspersen, P., and Jaeger, T., "Gas monitoring in the process industry using diode laser spectroscopy," *Applied Physics B: Lasers and Optics* **67**, 297–305 (1998).
- [2] Sigrist, M. W., [*Air Monitoring by Spectroscopic Techniques: Chemical Analysis*], Wiley, New York (1994).
- [3] Steffens, J., Landulfo, E., Guardani, R., do Nascimento, C. A. O., and Moreira, A., "The use of lidar as optical remote sensors in the assessment of air quality near oil refineries and petrochemical sites," in [*Proceedings of SPIE*], **7111**, 71110S (2008).
- [4] Steffens, J., Guardani, R., Landulfo, E., Jr., P. F. M., and Costa, R. F. D., "Study on correlations between lidar scattered light signal and air quality data in an industrial area," *Procedia Environmental Sciences* **4**, 95–102 (2011).
- [5] Measures, R. M., [*Laser Remote Sensing Fundamentals and Applications*], Krieger Publishing Company (1992).